

---

# Consistent and Distinctive: LLM Benchmark Efficiency via Maximum Independent Set Prompt Selection on Similarity Graphs

---

Denica Kjorvezir<sup>1,2</sup> Marko Djukanović<sup>3</sup> Ana Gjorgjevikj<sup>1</sup> Gjorgjina Cenikj<sup>1</sup>  
Tome Eftimov<sup>1,2</sup>

<sup>1</sup>Computer Systems Department, Jožef Stefan Institute, Ljubljana, Slovenia

<sup>2</sup>Jožef Stefan International Postgraduate School, Ljubljana, Slovenia

<sup>3</sup>Center for Astrophysics and Cosmology, University of Nova Gorica, Nova Gorica, Slovenia

---

**Abstract** Evaluating large language models (LLMs) across comprehensive benchmarks is expensive and time-consuming. We propose a graph-based prompt selection framework that models each benchmark as a similarity graph—nodes are prompts connected if their embedding-space distance falls above a configurable threshold—and applies Maximum Independent Set (MIS) algorithms to select a maximally diverse, non-redundant subset. We evaluate four MIS solvers (CPLEX, GREEDY, Online-MIS, ReduMIS) across six embedding models, three distance measures, six percentile thresholds, and four benchmarks (GPQA, IFEval, MMLU-Pro, Omni-MATH) covering 66 LLMs. Our central hypothesis—that repeated selection under different random seeds yields consistent LLM rankings that may also differ from the full-benchmark baseline—is strongly confirmed: Kendall’s  $W \geq 0.90$  in 99.2% of stochastic configurations (mean  $W = 0.997 \pm 0.008$ ), while at higher percentile thresholds selected subsets achieve 25–48% prompt reduction on average. Ranking divergence from the full benchmark ( $\rho < 0.95$ ) occurs in only 15.95% of configurations, concentrated at low thresholds ( $p_{10}$ – $p_{20}$ ) and benchmarks (GPQA, IFEval), identifying overly dense graphs as the primary failure mode.

---

## 1 Introduction

Rigorous evaluation of large language models (LLMs) requires benchmarks large enough to yield statistically reliable scores, yet small enough to be tractable at scale. Widely used benchmarks such as MMLU-Pro (Wang et al., 2024) and GPQA (Rein et al., 2023) contain hundreds to thousands of questions, incurring substantial inference costs for frontier LLMs and large-scale LLM leaderboards (Polo et al., 2024; Liang et al., 2022). Two related but distinct problems motivate this work.

The first is *efficiency*: can we select a compact, representative subset that preserves the relative ordering (ranking) of LLMs while substantially reducing evaluation overhead? The second is *coverage bias*: if the prompts of a benchmark are unevenly distributed in embedding space (overrepresenting certain semantic regions) the benchmark implicitly upweights model performance on those question types. For instance, if a reasoning benchmark contains disproportionately many similar chemistry questions, models that excel at chemistry receive inflated scores regardless of their general capability. This structural bias is invisible in aggregate performance metrics, yet it distorts rankings by amplifying performance on overrepresented facets of the capability space (Schilling-Wilhelmi et al., 2025; Truong et al., 2025).

Crucially, both problems share a single root cause: semantic redundancy among prompts. If many prompts are mutually close in embedding space, they *i*) waste evaluation budget and *ii*) overweight the capability facet they share. A method that eliminates semantic redundancy, therefore

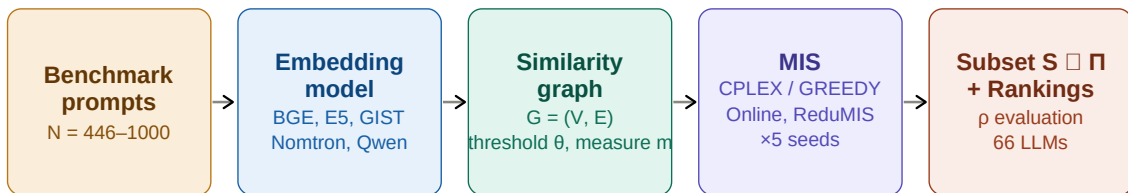


Figure 1: The MIS-based prompt selection pipeline. Prompts are encoded, a similarity graph is constructed using a distance threshold, and an MIS algorithm selects a maximally diverse subset for LLM evaluation.

addresses efficiency and coverage bias simultaneously. We propose modelling each benchmark as a prompt similarity graph  $G = (V, E)$ , where each prompt is a node ( $v \in V$ ) and an edge connects two prompts ( $(u, v) \in E$ ) if their embedding-space distance falls above a configurable threshold ( $d(e_u, e_v) \geq \theta$ ). A Maximum Independent Set (MIS) of this graph—the largest set of mutually non-adjacent nodes—corresponds to a maximally non-redundant subset: no two selected prompts are semantically close, and no semantic region is doubly counted. Figure 1 shows the full pipeline; Figure 2 illustrates the coverage correction effect. This design gives rise to our central hypothesis: *repeated MIS selection under different random seeds yields consistent LLM rankings—seeds agree with each other—while those rankings may differ from the full-benchmark baseline when the latter is coverage-biased.*

Our key contributions are: *i) A graph-theoretic prompt selection framework* that simultaneously addresses evaluation efficiency and coverage bias by selecting a maximally diverse, non-redundant subset via MIS, supporting four solvers, six embedding models, three distance measures, and six distance thresholds; *ii) Empirical confirmation of the consistency hypothesis* across 2,563 unique configurations and 66 LLMs on four benchmarks: Kendall’s  $W \geq 0.90$  in 99.2% of stochastic configurations (mean  $W = 0.997 \pm 0.008$ ), with only 25–48% prompt reduction at higher percentile thresholds; ranking divergence ( $\rho < 0.95$ ) is confined to 15.95% of configurations and is heavily concentrated at low thresholds ( $p_{10}-p_{20}$ ) and benchmarks (GPQA, IFEval), pinpointing overly dense graphs as the primary failure mode; and *iii) Detailed analysis of how selection quality and consistency vary* with algorithm, embedding model, distance measure, threshold, and benchmark.

## 2 Related Work

**LLM Benchmark Design and Efficiency:** The LLM benchmark landscape has grown rapidly, with evaluation scenarios spanning reasoning (Wang et al., 2024; Rein et al., 2023), instruction following (Zhou et al., 2023), and advanced mathematics (Cobbe et al., 2021; Hendrycks et al., 2021; Gao et al., 2025). Large-scale multi-dataset benchmarks such as Stanfords HELM (Liang et al., 2022), Chatbot Arena (Zheng et al., 2023), Open LLM Leaderboard by Hugging Face, and LiveBench (White et al., 2024) have become central infrastructure for standardized LLM evaluation across diverse scenarios and metrics.

Several works have noted that full benchmark evaluation is costly and that strategic subset selection can maintain ranking fidelity (Perlitz et al., 2023; Vivek et al., 2024). Recent Item Response Theory (IRT)-based work explores compressing LLM benchmarks without sacrificing reliability. Polo et al. (2024) show that small, IRT-curated subsets can reproduce full-benchmark results from 100 examples. Zhou et al. (2026) use item difficulty and discrimination to select informative instances and diagnose saturated benchmarks, while Truong et al. (2025) select maximally informative items relative to a model’s estimated ability. Zhang et al. (2026) cautions that subset-based prediction degrades at the frontier, where stronger models require extrapolation beyond observed

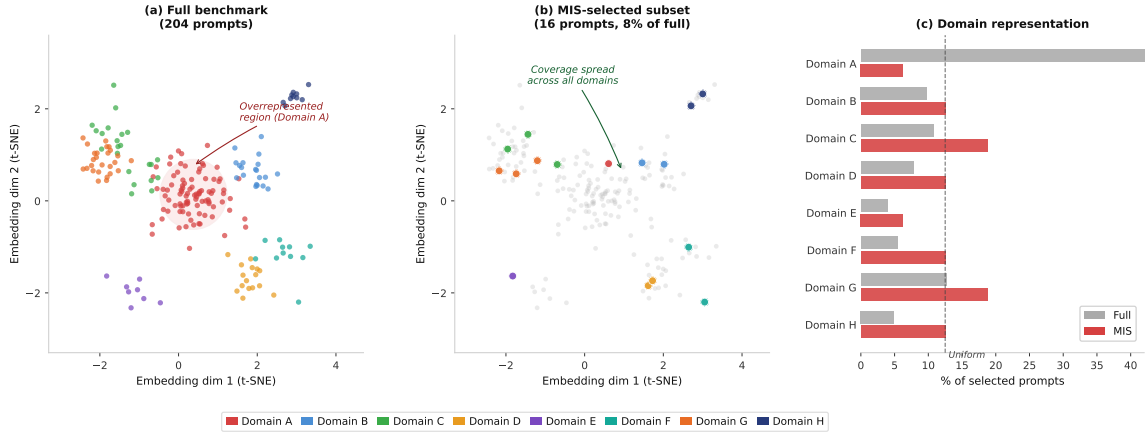


Figure 2: Embedding space coverage illustration. (a) Full benchmark: Domain A is overrepresented, biasing evaluation toward that capability facet. (b) MIS-selected subset: coloured points are selected; grey are excluded. Selection is spread uniformly across all domains. (c) Domain proportions before (grey) and after (coloured) MIS selection, approaching the uniform baseline (dashed). This coverage correction is a structural property of MIS, not a tunable parameter.

behavior. Chen et al. (2025) apply multidimensional IRT to embed LLMs and benchmark items in a shared latent space, improving both prediction and compression. Unlike these approaches, which require iterative model interaction, our method is *model-agnostic*, selecting prompts based solely on pairwise similarity.

**Coverage Bias in Benchmarks:** A less-studied problem is that benchmark prompts may be unevenly distributed in capability space. If a benchmark overrepresents certain question types, e.g., many paraphrases of the same underlying reasoning pattern, it implicitly amplifies those capabilities in the final score. Mizrahi et al. (2024) and Gururangan et al. (2018) show that dataset artefacts and distributional biases systematically favour particular model families. Our work formalises this concern geometrically: overrepresentation corresponds to prompt density in specific regions of embedding space, and MIS selection corrects it by construction—the independent set property ensures no region is doubly counted.

The graph-based selection methodology underlying our approach originates from SELECTOR (Cenikj et al., 2022), a framework addressing reproducibility and coverage bias in numerical optimization benchmarking. SELECTOR evaluates clustering and graph-theoretic heuristics—dominating sets and maximal independent sets (MIS) in a pairwise similarity graph—to construct non-redundant, coverage-uniform subsets that yield reproducible comparisons. This methodology has since been adopted in several follow-up studies: Eftimov et al. (2022) extend it to time series classification benchmarks, showing that coverage-uniform subsets yield more robust statistical conclusions than using all available datasets; Cenikj et al. (2024) apply it to deduplicate optimization instances before training a transformer-based algorithm selector; and Kostovska et al. (2023) apply it to select diverse algorithm portfolios from CMA-ES variants. However, all prior work constructs similarity graphs from domain-specific numeric representations using cosine similarity and a narrow set of fixed thresholds (0.80, 0.90, 0.95), with only two graph algorithms evaluated. Our work extends SELECTOR to natural language prompts, employing nine embedding methods, three distance measures, and six data-driven thresholds per embedding distance combination, and evaluating four MIS solvers across four NLP benchmarks and 66 LLMs. We show that the structural coverage guarantees established in optimization benchmarking transfer to LLM evaluation.

### 3 Methodology

Figure 1 shows the full methodology pipeline.

**Embedding Construction:** To compare prompts geometrically, each prompt  $p_i \in \Pi$  must first be mapped to a fixed-dimensional vector representation. An embedding model  $f : \mathcal{P} \rightarrow \mathbb{R}^d$  encodes the semantic content of a prompt into a dense vector  $e_i = f(p_i)$ , where  $d$  is the model-specific embedding dimension. Embeddings are designed so that semantically similar inputs map to nearby points in  $\mathbb{R}^d$ , enabling distance-based reasoning about prompt redundancy. Proximity is measured via a distance function  $m$  (e.g., cosine or Euclidean distance) applied to normalized vectors.

**Similarity Graph Construction:** Given the prompt embeddings  $\{e_1, \dots, e_N\}$ , we construct a similarity graph  $G = (V, E)$  that explicitly captures redundancy relationships among prompts. Each prompt  $p_i$  is represented by a node  $v_i \in V$ . An undirected edge  $(v_i, v_j) \in E$  is added whenever the pairwise distance between embeddings exceeds a predefined threshold, i.e.,  $d(e_i, e_j) \geq \theta$ . The threshold  $\theta$  controls the strictness of similarity enforcement. Smaller threshold values produce denser graphs by connecting prompts that differ even moderately, whereas larger thresholds generate sparser graphs by connecting only highly similar prompts. Under this construction, an independent set corresponds to a subset of prompts whose pairwise distances remain below the threshold  $\theta$ , thereby ensuring semantic coherence and redundancy preservation within the selected subset. The resulting graph therefore, serves as the structural foundation for the deduplication and subset selection procedures described in the following sections.

**Maximum Independent Set:** With the similarity graph  $G$  in hand, we cast benchmark deduplication as a Maximum Independent Set (MIS) problem: find the largest subset  $S \subseteq V$  such that no two nodes in  $S$  share an edge, i.e., two selected prompts are mutually similar under threshold  $\theta$ . For any two selected prompts  $p_i, p_j \in S$ ,  $d(e_i, e_j) < \theta$  by the independence constraint. This means the selected subset cannot over-concentrate in any embedding-space region of radius  $\theta/2$ : at most one prompt can be drawn from any such region. In contrast, random or stratified sampling provides no such guarantee. Importantly, since all prompts in an MIS satisfy pairwise distance constraints below  $\theta$ , the resulting subset provides a compressed semantic representation of a larger benchmark region. This enables benchmark reduction through representative prompt selection while preserving semantic consistency. Consequently, changes in downstream LLM rankings are not merely a consequence of random sampling variation, but reflect differences in the semantic structure retained after compression.

**Evaluation Metrics:** Having obtained a deduplicated subset  $S$  via MIS, we assess both its effect on LLM rankings and the internal stability of stochastic solvers. For each selected subset  $S$  we compute mean LLM accuracy restricted to  $S$ , yielding ranking  $\sigma(S)$ , and compare to the full-benchmark ranking  $\sigma(\Pi)$  using Spearman’s rank correlation coefficient  $\rho$ . For stochastic MIS algorithms, internal concordance across all repeated seeds is measured by Kendall’s  $W$  (Coefficient of Concordance):

$$W = \frac{\mathcal{S}}{m^2(n^3 - n)/12 - m \sum_j T_j} \tag{1}$$

where  $m$  is the number of seeds,  $n$  is the number of LLMs,  $\mathcal{S} = \sum_i (R_i - \bar{R})^2$  is the sum of squared deviations of per-item rank sums  $R_i$  from their mean, and  $T_j = \sum t(t^2 - 1)/12$  is the tie correction for judge  $j$ .  $W \in [0, 1]$ , with  $W = 1$  indicating perfect agreement across all seeds simultaneously. Following Landis and Koch (1977),  $W \geq 0.90$  is considered near-perfect concordance,  $W \geq 0.80$  substantial, and  $W < 0.60$  poor; all results reported below use  $W \geq 0.90$  as the high-concordance threshold.

Table 1: Benchmark statistics.  $|P|$  = prompts;  $|M|$  = #LLMs; Acc. min/max = accuracy range.

Dataset	$ P $	$ M $	Acc. min	Acc. max	Top-1 model
GPQA	446	66	0.168	0.803	Gemini 3 Pro (thinking)
IFEval	541	66	0.567	0.951	Grok-3 Mini
MMLU-Pro	1,000	66	0.169	0.903	Gemini 3 Pro (thinking)
Omni-MATH	1,000	66	0.072	0.722	GPT-5 Mini (thinking)

## 4 Experimental Setup

**Benchmarks:** We evaluate on four benchmarks from the HELM Capabilities leaderboard spanning knowledge-intensive QA (MMLU-Pro (Wang et al., 2024), GPQA (Rein et al., 2023)), instruction following (IFEval (Zhou et al., 2023)), and mathematical reasoning (Omni-MATH (Gao et al., 2025)). We restrict to single-turn benchmarks to ensure all instances can be represented as independent text embeddings. Table 1 summarizes the four benchmarks evaluated across a fixed set of 66 frontier and open LLMs (listed in Appendix A), including GPT, Claude, Gemini (Team et al., 2023), Llama (Grattafiori et al., 2024), Qwen3 (Yang et al., 2025), DeepSeek (Liu et al., 2024), and Mistral (Jiang et al., 2023), enabling consistent comparison of ranking agreement across tasks. All scores were collected from the HELM Capabilities leaderboard as of May 2025; since HELM scores may reflect differing prompting strategies across model families (e.g., zero-shot vs. few-shot), our comparisons are relative to HELM-reported baselines rather than a controlled prompting protocol. The benchmarks differ in score distribution: MMLU-Pro and GPQA aggregate binary per-item correctness, yielding smooth accuracy estimates with strong rank separability, while IFEval and Omni-MATH produce discretized or bounded score distributions with reduced granularity. We therefore use rank-based metrics (Spearman’s  $\rho$ , Kendall’s W), both robust to discretization effects.

**Sentence Embeddings:** We construct sentence-level embeddings using six models spanning two regimes: three small encoder-based models (*bge-large-en-v1.5* (Xiao et al., 2024), *e5-large* (Wang et al., 2022), *GIST-small-Embedding-v0* (Solatorio, 2024)) and three large decoder-based models (*Llama-Embed-Nemotron-8B* (Babakhin et al., 2025), *Qwen3-4B*, and *Qwen3-8B* (Zhang et al., 2025)), capturing both contrastive encoder training dynamics and large-scale generative embedding representations. Encoder models operate under a  $\sim 512$ -token context window; we therefore apply length-weighted averaging over non-overlapping 510-token chunks to avoid truncation artifacts. Decoder-based models support up to 4,096 tokens, sufficient to encode all benchmark prompts in full (maximum length 2,278.5 tokens). We additionally evaluate a chunked variant for decoder models using overlapping windows (stride 256) to enable a controlled comparison between full-sequence and segmented representations. All models use attention-mask-weighted mean pooling over final hidden states followed by L2 normalization. This yields three complementary embedding views: encoder-based chunked, decoder-based full-sequence, and decoder-based chunked, allowing us to assess the impact of architecture and context handling on similarity structure and ranking stability.

**Distance measures and thresholds:** We evaluate three proximity measures for constructing similarity graphs: cosine similarity, Pearson correlation distance, and standardized Euclidean (*euclidean*) distance, each capturing different geometric and statistical properties of the embedding space. Graph construction is controlled via a threshold  $\theta$  defined as a percentile of the empirical pairwise distance distribution, estimated from 10,000 randomly sampled embedding pairs. We consider thresholds ranging from  $p_{10}$  to  $p_{95}$ , providing a normalised, model-independent way to control graph sparsity across datasets and embedding models with potentially different distance scales. Distance distributions vary substantially across embedding models and measures (Appendix B, Figures 5–7), motivating percentile-based thresholding over fixed absolute values.

Table 2: Per-algorithm summary.  $\rho$  = mean Spearman correlation with the full-benchmark ranking;  $\rho_{\text{std}}$  = standard deviation across configurations (benchmark, embedding model, distance measure, threshold);  $\rho \geq 0.95$  = fraction of configurations achieving high rank agreement;  $W$  = Kendall’s coefficient of concordance across seed rankings;  $W_{\text{std}}$  = standard deviation of  $W$  across seeds;  $|S|$  = mean selected prompt subset size.  $W$  and  $W_{\text{std}}$  are undefined (–) for deterministic algorithms CPLEX and GREEDY, which produce a single fixed output per configuration. **Bold**: best stochastic consistency metrics.

Algorithm	$\rho$ (mean)	$\rho_{\text{std}}$	$\rho \geq 0.95$ (%)	$W$	$W_{\text{std}}$	$ S $
CPLEX	0.968	0.060	84.3	–	–	331.9
GREEDY	0.968	0.063	84.3	–	–	330.2
Online-MIS	0.967	0.060	84.3	0.9963	0.0102	327.9
ReduMIS	0.968	0.060	83.8	<b>0.9976</b>	<b>0.0076</b>	330.7

**MIS Algorithms:** We employ four MIS solvers spanning exact and heuristic approaches. **CPLEX** Anand et al. (2017) solves the Maximum Independent Set (MIS) problem exactly via an Integer Linear Programming (ILP) formulation, using branch-and-bound and branch-and-cut strategies with presolve reductions and cut generation to prove optimality. **GREEDY** is a deterministic heuristic that iteratively selects the lowest-degree vertex in the residual graph, adds it to the independent set, and removes it along with its neighbours. It offers no optimality guarantee but scales well to large graphs. **Online-MIS** (Dahlum et al., 2016) is a randomised streaming heuristic that processes vertices in a random order, accepting each vertex if none of its already-accepted neighbours are in the solution. We run five independent seeds per instance to reduce variance. **ReduMIS** (Lamm et al., 2017) combines graph kernelisation and reduction rules with stochastic local search, substantially shrinking the graph before exploring the remaining solution space. Solutions are lifted back to the original graph; five seeds are used per instance. On a graph with  $n = 1000$  nodes, CPLEX requires approximately 30–120 seconds depending on density, ReduMIS and Online-MIS 600 seconds, and GREEDY under one second.

**Configuration Space:** The full grid comprises 2592 unique configurations (embedding model, distance measure, threshold, optimization algorithm). We have ended up with 2,563 unique combinations out of 2,592. A few combinations are missing relative to a full cross-product, suggesting a handful of runs did not complete. Stochastic optimization algorithms are run with five seeds.

## 5 Results

**Overall Performance by Algorithm:** Table 2 shows that all algorithms achieve nearly identical Spearman rank correlation with the full-benchmark ordering ( $\rho \approx 0.967$ – $0.968$ ), indicating that global ranking structure is largely invariant to solver choice. The results are aggregated per optimization algorithm, i.e., across all combinations of benchmarks, embedding models, distance measures, and thresholds. The fraction of high-correlation configurations remains stable across methods ( $\rho \geq 0.95 \approx 84\%$ ), suggesting that performance differences primarily reflect alignment with using full baselines rather than changes in overall rank fidelity. Both stochastic optimization methods, ReduMIS and Online-MIS, achieve the strongest overall concordance ( $W = 0.9976$  vs.  $0.9963$ ), indicating that rankings achieved across seeds are robust and stable.

**Per-Dataset Analysis:** Table 3 reveals clear but moderate variation across benchmarks. The results are aggregated for each benchmark and stochastic optimization algorithm across all combinations of embedding models, distance measures, and thresholds. GPQA, MMLU-Pro, and Omni-MATH exhibit high ranking preservation when using them as full benchmarks ( $\rho \approx 0.971$ – $0.993$ ) and near-perfect concordance ( $W \approx 0.997$ – $0.999$ ). IFEval is the most challenging benchmark, with noticeably lower ranking agreement than the other three benchmarks but still higher correlation

Table 3: Per-dataset and per-algorithm results for stochastic algorithms.  $\rho$  = mean Spearman correlation with the full-benchmark ranking;  $\rho_{\text{std}}$  = standard deviation across configurations;  $W$  = Kendall’s coefficient of concordance;  $W_{\text{std}}$  = standard deviation of  $W$  across seeds;  $|S|$  = mean selected subset size.

Dataset	Algorithm	$\rho$ (mean)	$\rho_{\text{std}}$	$W$	$W_{\text{std}}$	$ S $
GPQA	Online-MIS	0.971	0.039	0.9973	0.0037	216.1
GPQA	ReduMIS	0.972	0.038	0.9983	0.0025	216.5
IFEval	Online-MIS	0.921	0.097	0.9907	0.0184	237.0
IFEval	ReduMIS	0.920	0.097	0.9941	0.0142	237.2
MMLU-Pro	Online-MIS	0.987	0.014	0.9985	0.0022	454.7
MMLU-Pro	ReduMIS	0.987	0.014	0.9989	0.0019	456.0
Omni-MATH	Online-MIS	0.993	0.010	0.9990	0.0019	413.1
Omni-MATH	ReduMIS	0.993	0.010	0.9992	0.0017	420.8

Table 4: Effect of similarity threshold averaged across all algorithms (CPLEX, GREEDY, Online-MIS, ReduMIS) and all embedding configurations (6 models  $\times$  3 distance measures  $\times$  4 benchmarks).  $\rho$  = mean Spearman correlation with the full benchmark ranking;  $\rho_{\text{std}}$  = standard deviation across configurations;  $W$  = Kendall’s coefficient of concordance;  $W_{\text{std}}$  = standard deviation of  $W$ ;  $|S|$  = mean selected subset size; Reduction = relative reduction in selected set size vs. full benchmark. Higher thresholds consistently improve ranking quality with diminishing returns beyond p80.

Threshold	$\rho$	$\rho_{\text{std}}$	$W$	$W_{\text{std}}$	$ S $	Reduction (%)
p10	0.905	0.100	0.9901	0.0180	69.7	88.2–92.5
p20	0.942	0.067	0.9948	0.0092	117.7	79.8–87.2
p50	0.974	0.031	0.9983	0.0025	245.4	62.0–70.1
p80	0.992	0.010	0.9993	0.0011	429.1	37.2–44.9
p90	0.996	0.004	0.9996	0.0006	525.0	25.0–32.9
p95	0.997	0.002	0.9996	0.0006	593.3	17.2–23.3

( $\rho \approx 0.920$ – $0.921$ ) and high concordance ( $W \approx 0.991$ – $0.994$ ). This reflects its instruction-following structure, where embedding similarity is less predictive of downstream performance similarity, leading to higher variability across sampled subsets while still maintaining high concordance overall.

**Effect of Threshold:** Table 4 quantifies the effect of the similarity threshold. As  $\theta$  increases from p10 to p95, both  $\rho$  and  $W$  improve monotonically, while the mean selected set size grows from  $\sim 70$  to  $\sim 593$  prompts, corresponding to a reduction from approximately 88–93% at p10 to 17–23% at p95. At very aggressive thresholds (p10–p20), ranking quality with the full benchmarks is already reasonably high ( $\rho \approx 0.905$ – $0.942$ ,  $W \approx 0.990$ – $0.995$ ), indicating strong robustness even under extreme pruning. However, these results are aggregated across all combinations of benchmarks, optimization algorithms, embedding methods, and distance measures. As a result, some specific combinations exhibit lower correlation values, which are discussed later. The p80 threshold provides a strong trade-off between efficiency and fidelity, achieving near-perfect ranking preservation ( $\rho = 0.992$ ,  $W = 0.999$ ) with a 37–45% reduction. Beyond p80, gains in ranking quality are marginal, while reductions in set size diminish rapidly, indicating a clear regime of diminishing returns.

**Embedding Model and Distance Measure:** Table 5 compares embedding models and distance measures. Overall, large models consistently achieve higher values than the small models in both

Table 5: Mean Spearman correlation ( $\rho$ ) and Kendall’s coefficient of concordance ( $W$ ) by embedding model and distance measure (stochastic algorithms only). S/L denote small encoder-based and large decoder-based models respectively. **Bold**: best  $W$ .

Model	Measure	$\rho$	$W$
bge (S)	correlation	0.954	0.9969
bge (S)	cosine	0.952	0.9966
bge (S)	seuclidean	0.951	0.9971
e5 (S)	correlation	0.964	0.9934
e5 (S)	cosine	0.963	0.9936
e5 (S)	seuclidean	0.962	0.9940
gist (S)	correlation	0.953	0.9932
gist (S)	cosine	0.952	0.9937
gist (S)	seuclidean	0.957	0.9947
nemotron (L)	correlation	0.973	0.9982
nemotron (L)	cosine	0.973	0.9985
nemotron (L)	seuclidean	0.972	0.9980
qwen4b (L)	correlation	0.970	0.9972
qwen4b (L)	cosine	0.969	0.9973
qwen4b (L)	seuclidean	0.979	0.9978
qwen8b (L)	correlation	0.970	0.9982
qwen8b (L)	cosine	0.970	0.9980
qwen8b (L)	seuclidean	0.983	<b>0.9993</b>

ranking agreement with the full benchmarks and robustness across different seeds. Among all configurations, qwen8b with standardized Euclidean distance achieves the highest concordance, reaching  $W = 0.9993$ , indicating near-perfect reproducibility of selected subsets. Across models, Euclidean-based distance (seuclidean) is generally competitive or slightly stronger than cosine and correlation, particularly for larger models, where all measures converge toward high agreement regimes ( $W \geq 0.997$ ).

## 6 Hypothesis Analysis

**The W-high /  $\rho$ -varies Hypothesis:** Figure 3 plots Kendall  $W$  against Spearman  $\rho$  for all stochastic configurations. The hypothesis predicts points concentrated in the upper half ( $W$  high, seeds agree) distributed across the full  $x$ -range ( $\rho$  varies). This is strongly confirmed: i) Kendall’s  $W \geq 0.90$  in 99.2% of configurations; the two failing cases (both from the *E5* embedding model on IFEval using ONLINE-MIS at the  $p_{10}$  threshold under cosine and Pearson correlation distances) arise from the same combination of an overly dense graph and a stochastic solver; ii) Of the 2,563 tested configurations (benchmark  $\times$  embedding model  $\times$  distance measure  $\times$  threshold  $\times$  solver), 409 (15.95%) yield a Spearman’s  $\rho < 0.95$ . These failures are heavily concentrated in GPQA (28.4%) and IFEval (64.8%), with far fewer in MMLU-Pro (3.9%) and Omni-MATH (2.9%), reflecting the greater score discretisation and ranking instability of the former two benchmarks. Failures are similarly concentrated at low similarity thresholds: 56.7% occur at  $p_{10}$  and 28.6% at  $p_{20}$ , dropping sharply to 13.2% at  $p_{50}$  and 1.5% at  $p_{80}$ , indicating that overly dense graphs—which retain too few representative prompts—are the primary source of ranking degradation; iii) Both conditions (consistent + distinctive): 16.2% of configurations, and iv) Consistent + same as baseline: 83.6% of configurations. Larger decoder-based models (*Nemotron-8B*, *Qwen-4B*, *Qwen-8B*) yield a higher proportion of representative configurations ( $\rho \geq 0.95$ : 85.3–87.5%) compared to the smaller encoder-based models

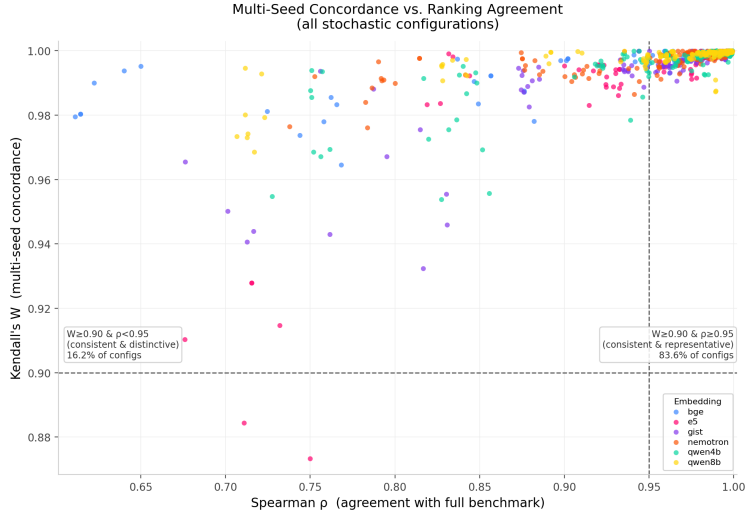


Figure 3: Kendall’s  $W$  (seed concordance) vs. Spearman  $\rho$  (agreement with full baseline) for all stochastic configurations, coloured by embedding model. Reference lines at  $W = 0.90$ ,  $\rho = 0.95$  define four quadrants. Most points fall in the upper region ( $W \geq 0.99$  in 99.2% of configs), with substantial spread along the  $x$ -axis (varying  $\rho$ ), confirming the hypothesis.

(*BGE*, *E5*, *GIST*; 75.7–80.4%; Table 6), suggesting that richer embedding representations better preserve the ranking structure under graph-based compression. Table 8 (Appendix G) slices the same points by benchmark, revealing starker differences: IFEval yields 39.8% distinctive subsets versus just 1.9% for Omni-MATH, reflecting how semantically clustered each benchmark’s prompts are in embedding space.

Table 6: Per-embedding model breakdown of configuration outcomes.

Embedding	Distinctive ( $W \geq 0.90$ & $\rho < 0.95$ )	Same as baseline ( $W \geq 0.90$ & $\rho \geq 0.95$ )
<i>BGE</i>	19.6%	80.4%
<i>E5</i>	19.4%	79.2%
<i>GIST</i>	24.3%	75.7%
<i>Nemotron</i>	13.8%	86.2%
<i>Qwen-4B</i>	14.7%	85.3%
<i>Qwen-8B</i>	12.5%	87.5%

**Prompt Reduction vs. Quality:** Figure 4 shows the relationship between fraction of prompts selected and both  $\rho$  and  $W$  across benchmarks in combination with the stochastic optimization algorithm. All benchmarks show a positive correlation between selection size and ranking quality, but with benchmark-specific slopes: MMLU-Pro and Omni-MATH maintain high  $\rho$  even with small subsets, while IFEval requires larger fractions to achieve good quality. Similar patterns are visible for the consistency of the rankings across different seeds.

**Case Study: Rank Shift Visualization:** Figure 8 (Appendix C) illustrates the hypothesis concretely for a single configuration (Online-MIS, IFEval, Qwen4b embedding, cosine distance, p20 threshold). The heatmap shows the rank deviation of each of the top-22 baseline models across 5 seeds and the full-dataset baseline (rightmost column). Seed columns exhibit similar colour patterns ( $W = 0.972$ : consistent), while the selected subset shifts some models relative to the full-benchmark ranking ( $\rho = 0.820$ : distinctive). This specific example represents an extreme case illustrating maximum

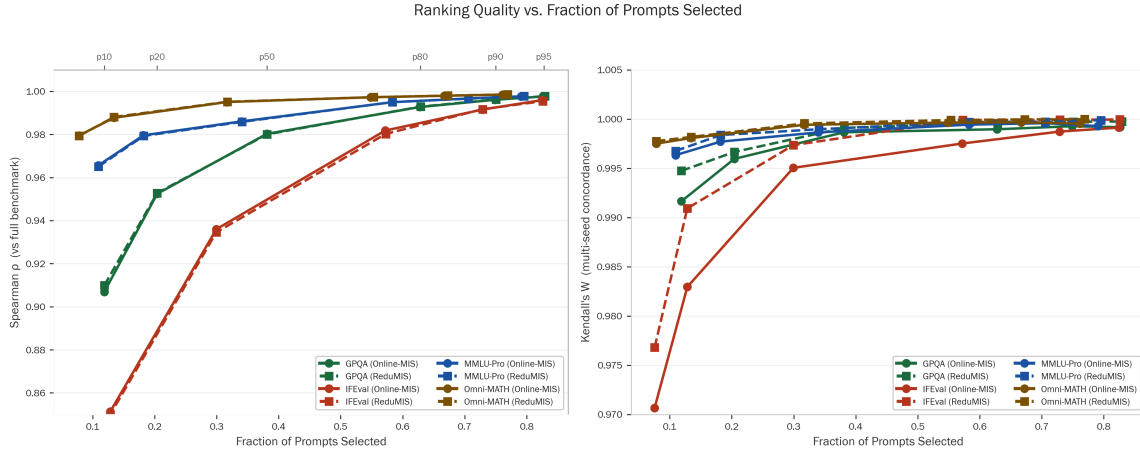


Figure 4: Agreement with full baseline ( $\rho$ , left) and seed consistency ( $W$ , right) as a function of the fraction of prompts selected, by dataset. Trend lines fitted per benchmark and stochastic optimization algorithm. MMLU-Pro and Omni-MATH achieve high quality even with small fractions (p10, p20, etc); IFEval requires larger subsets for comparable quality.

distinction, where the MIS selection focuses on a restricted subset of instruction-following tasks, revealing a markedly different model capability profile—an extreme but illustrative instance of the distinctive-consistent trade-off.

## 7 Discussion

Our results establish MIS-based prompt selection as a principled, efficient approach to LLM benchmarking that simultaneously addresses two problems: evaluation cost and coverage bias. Practical recommendations: (1) Use threshold p80 for a strong balance of quality and reduction. (2) ReduMIS is the recommended stochastic solver: superior  $W$ , near-optimal solutions. (3) Large embedding models provide modest gains; small models (BGE+correlation) are viable when compute is limited. (4) IFEval requires careful calibration—instruction-following benchmarks with dense similarity graphs demand higher thresholds.

**Recommended configuration for practitioners:** For most benchmarks, we recommend: ReduMIS solver + qwen8b embedding + standardized Euclidean distance + p80 threshold. This combination achieves  $W = 1.000$  and  $\rho = 0.9959$ .

**Reinterpreting  $\rho < 0.95$  as a feature, not a flaw:** A common concern with subset evaluation is that a lower Spearman  $\rho$  indicates poor quality. Our framework reframes this: when the full benchmark is coverage-biased,  $\rho < 0.95$  is expected and desirable. The MIS subset down-weights overrepresented capability facets and amplifies discriminative signal from under-sampled regions, yielding a different—but not worse—ranking. IFEval’s with small thresholds ( $p_{10}$ ,  $p_{20}$ ) notably low  $\rho$  ( $\approx 0.920$  for stochastic algorithms) is the most extreme case: its dense embedding clusters mean that MIS selection operates on a very different capability distribution than the full set, surfacing a complementary perspective. Concordance remains high ( $W \approx 0.990$ – $0.994$ ), confirming that all five seeds agree on this alternative view.

**Coverage uniformity as a diagnostic:** The degree distribution of the full benchmark graph—how many similar prompts surround each prompt—directly quantifies its coverage bias. Benchmarks with high-degree hubs (many near-duplicate prompts) are most prone to bias and benefit most from MIS selection. Future work will report benchmark graph statistics for different embedding models, distance measures, and threshold settings alongside accuracy metrics, enabling transparent assessment of the structural biases introduced by benchmark construction.

## 8 Conclusion

We introduced an MIS framework for efficient, coverage-unbiased LLM benchmark evaluation, formalised as a graph-theoretic problem on prompt similarity graphs. The framework addresses two problems simultaneously: (1) reducing evaluation cost, with 25–48% prompt reduction at higher percentile thresholds, and (2) correcting coverage bias by ensuring no semantic region is overrepresented. Across four benchmarks, 66 LLMs, four algorithms, six embedding models, three distance measures, and six thresholds, the consistency hypothesis is strongly confirmed:  $W \geq 0.90$  in 99.2% of stochastic configurations (mean  $W = 0.997 \pm 0.008$ ). Ranking divergence from the full benchmark ( $\rho < 0.95$ ) occurs in only 15.95% of configurations and is reframed as either a coverage correction effect or a diagnosable failure: failures are heavily concentrated at low thresholds ( $p_{10}$ – $p_{20}$ ) and discretised benchmarks (GPQA, IFEval), identifying overly dense graphs—which retain too few representative prompts—as the primary source of ranking degradation. ReduMIS emerges as the recommended algorithm ( $W = 0.997$ ). Future work will explore adaptive threshold selection, IRT integration, and coverage-aware ensemble evaluation.

### Limitations

This study does not enforce sub-domain coverage beyond what the embedding captures; domains not well-separated in embedding space may still be conflated by MIS selection. The coverage-correction argument assumes the embedding model faithfully reflects semantic similarity relevant to the tested capability—an assumption that may not hold for highly domain-specific benchmarks. Results reflect a snapshot of 66 LLMs as of mid-2025. Large embedding models require significant GPU memory. All benchmarks are English-language; applicability to multilingual or code-centric benchmarks remains to be validated.

### Reproducibility.

The source code and data are available upon request from the authors.

### Acknowledgement

This work is funded by the Slovenian Research and Innovation Agency under program grant P2-0098, and project grants No. J2-70078 and No. GC-0001; and by the European Union under Grant Agreement 101187010 (HE ERA Chair AutoLearn-SI) and Grant Agreement 101211695 (HE MSCA-PF AutoLLMSelect). This work is also co-funded by the European Unions Horizon Europe research and innovation program under the Marie Skłodowska-Curie COFUND Postdoctoral Programme (grant agreement No. 101081355 – SMASH), and by the Republic of Slovenia and the European Union through the European Regional Development Fund.

### References

- Anand, R., Aggarwal, D., and Kumar, V. (2017). A comparative analysis of optimization solvers. *Journal of Statistics and Management Systems*, 20(4):623–635.
- Babakhin, Y., Osmulski, R., Ak, R., Moreira, G., Xu, M., Schifferer, B., Liu, B., and Oldridge, E. (2025). Llama-embed-nemotron-8b: A universal text embedding model for multilingual and cross-lingual tasks. *arXiv preprint arXiv:2511.07025*.
- Cenikj, G., Dieter Lang, R., Petrus Engelbrecht, A., Doerr, C., Koroec, P., and Eftimov, T. (2022). SELECTOR: Selecting a Representative Benchmark Suite for Reproducible Statistical Comparison. In *Proc. of Genetic and Evolutionary Computation Conference (GECCO)*.

- Cenikj, G., Petelin, G., and Eftimov, T. (2024). Transoptas: Transformer-based algorithm selection for single-objective optimization. In *Proceedings of the Genetic and Evolutionary Computation Conference Companion, GECCO '24 Companion*, page 403406, New York, NY, USA. Association for Computing Machinery.
- Chen, J., Wang, C., Zhang, G., Ye, P., Bai, L., Hu, W., Qu, Y., and Hu, S. (2025). Learning compact representations of llm abilities via item response theory. *arXiv preprint arXiv:2510.00844*.
- Cobbe, K., Kosaraju, V., Bavarian, M., Chen, M., Jun, H., Kaiser, L., Plappert, M., Tworek, J., Hilton, J., Nakano, R., et al. (2021). Training verifiers to solve math word problems. *arXiv preprint arXiv:2110.14168*.
- Dahlum, J., Lamm, S., Sanders, P., Schulz, C., Strash, D., and Werneck, R. F. (2016). Accelerating local search for the maximum independent set problem. In *15th International Symposium on Experimental Algorithms SEA*, volume 9685 of *Lecture Notes in Computer Science*, pages 118–133. Springer.
- Eftimov, T., Petelin, G., Cenikj, G., Kostovska, A., Ispirova, G., Koroec, P., and Bogatinovski, J. (2022). Less is more: Selecting the right benchmarking set of data for time series classification. *Expert Systems with Applications*, 198:116871.
- Gao, B., Song, F., Yang, Z., Cai, Z., Miao, Y., Dong, Q., Li, L., Ma, C., Chen, L., Tang, Z., et al. (2025). Omni-math: A universal olympiad level mathematic benchmark for large language models. In *International Conference on Learning Representations*, volume 2025, pages 100540–100569.
- Grattafiori, A., Dubey, A., Jauhri, A., Pandey, A., Kadian, A., Al-Dahle, A., Letman, A., Mathur, A., Schelten, A., Vaughan, A., et al. (2024). The llama 3 herd of models. *arXiv preprint arXiv:2407.21783*.
- Gururangan, S., Swayamdipta, S., Levy, O., Schwartz, R., Bowman, S., and Smith, N. A. (2018). Annotation artifacts in natural language inference data. In *Proceedings of the 2018 Conference of the North American Chapter of the Association for Computational Linguistics: Human Language Technologies*, pages 107–112.
- Hendrycks, D., Burns, C., Kadavath, S., Arora, A., Basart, S., Tang, E., Song, D., and Steinhardt, J. (2021). Measuring mathematical problem solving with the math dataset. *arXiv preprint arXiv:2103.03874*.
- Jiang, A. Q., Sablayrolles, A., Mensch, A., Bamford, C., Chaplot, D. S., Casas, D., Bressand, F., Lengyel, G., Lample, G., Saulnier, L., et al. (2023). Mistral 7b. *arXiv preprint arXiv:2310.06825*.
- Kostovska, A., Cenikj, G., Vermetten, D., Jankovic, A., Nikolikj, A., Skvorc, U., Korosec, P., Doerr, C., and Eftimov, T. (2023). Ps-aas: Portfolio selection for automated algorithm selection in black-box optimization. In *International Conference on Automated Machine Learning*, pages 11–1. PMLR.
- Lamm, S., Sanders, P., Schulz, C., Strash, D., and Werneck, R. F. (2017). Finding near-optimal independent sets at scale. *J. Heuristics*, 23(4):207–229.
- Landis, J. R. and Koch, G. G. (1977). The measurement of observer agreement for categorical data. *biometrics*, pages 159–174.
- Liang, P., Bommasani, R., Lee, T., Tsipras, D., Soylu, D., Yasunaga, M., Zhang, Y., Narayanan, D., Wu, Y., Kumar, A., et al. (2022). Holistic evaluation of language models. *arXiv preprint arXiv:2211.09110*.

- Liu, A., Feng, B., Xue, B., Wang, B., Wu, B., Lu, C., Zhao, C., Deng, C., Zhang, C., Ruan, C., et al. (2024). Deepseek-v3 technical report. *arXiv preprint arXiv:2412.19437*.
- Mizrahi, M., Kaplan, G., Malkin, D., Dror, R., Shahaf, D., and Stanovsky, G. (2024). State of what art? a call for multi-prompt LLM evaluation. *Transactions of the Association for Computational Linguistics*, 12:933–949.
- Perlitz, Y., Bandel, E., Gera, A., Arviv, O., Ein-Dor, L., Shnarch, E., Slonim, N., Shmueli-Scheuer, M., and Choshen, L. (2023). Efficient benchmarking of language models. *arXiv preprint arXiv:2308.11696*.
- Polo, F. M., Weber, L., Choshen, L., Sun, Y., Xu, G., and Yurochkin, M. (2024). tinybenchmarks: evaluating llms with fewer examples. *arXiv preprint arXiv:2402.14992*.
- Rein, D., Hou, B. L., Stickland, A. C., Petty, J., Pang, R. Y., Dirani, J., Michael, J., and Bowman, S. R. (2023). Gpqa: A graduate-level google-proof q&a benchmark. *arXiv preprint arXiv:2311.12022*.
- Schilling-Wilhelmi, M., Alampara, N., and Jablonka, K. M. (2025). Lifting the benchmark iceberg with item-response theory. In *AI for Accelerated Materials Design-ICLR 2025*.
- Solatorio, A. V. (2024). Gistembed: Guided in-sample selection of training negatives for text embedding fine-tuning. *arXiv preprint arXiv:2402.16829*.
- Team, G., Anil, R., Borgeaud, S., Alayrac, J.-B., Yu, J., Soricut, R., Schalkwyk, J., Dai, A. M., Hauth, A., Millican, K., et al. (2023). Gemini: a family of highly capable multimodal models. *arXiv preprint arXiv:2312.11805*.
- Truong, S., Tu, Y., Liang, P., Li, B., and Koyejo, S. (2025). Reliable and efficient amortized model-based evaluation. *arXiv preprint arXiv:2503.13335*.
- Vivek, R., Ethayarajh, K., Yang, D., and Kiela, D. (2024). Anchor points: Benchmarking models with much fewer examples. In *Proceedings of the 18th Conference of the European Chapter of the Association for Computational Linguistics (Volume 1: Long Papers)*, pages 1576–1601.
- Wang, L., Yang, N., Huang, X., Jiao, B., Yang, L., Jiang, D., Majumder, R., and Wei, F. (2022). Text embeddings by weakly-supervised contrastive pre-training. *arXiv preprint arXiv:2212.03533*.
- Wang, Y., Ma, X., Zhang, G., Ni, Y., Chandra, A., Guo, S., Ren, W., Arulraj, A., He, X., Jiang, Z., et al. (2024). Mmlu-pro: A more robust and challenging multi-task language understanding benchmark. *Advances in Neural Information Processing Systems*, 37:95266–95290.
- White, C., Dooley, S., Roberts, M., Pal, A., Feuer, B., Jain, S., Shwartz-Ziv, R., Jain, N., Saifullah, K., Naidu, S., et al. (2024). Livebench: A challenging, contamination-free llm benchmark. *arXiv preprint arXiv:2406.19314*, 4:2.
- Xiao, S., Liu, Z., Zhang, P., Muennighoff, N., Lian, D., and Nie, J.-Y. (2024). C-pack: Packed resources for general chinese embeddings. In *Proceedings of the 47th international ACM SIGIR conference on research and development in information retrieval*, pages 641–649.
- Yang, A., Li, A., Yang, B., Zhang, B., Hui, B., Zheng, B., Yu, B., Gao, C., Huang, C., Lv, C., et al. (2025). Qwen3 technical report. *arXiv preprint arXiv:2505.09388*.
- Zhang, G., Dorner, F. E., and Hardt, M. (2026). How benchmark prediction from fewer data misses the mark. *Advances in Neural Information Processing Systems*, 38:135638–135678.

Zhang, Y., Li, M., Long, D., Zhang, X., Lin, H., Yang, B., Xie, P., Yang, A., Liu, D., Lin, J., et al. (2025). Qwen3 embedding: Advancing text embedding and reranking through foundation models. *arXiv preprint arXiv:2506.05176*.

Zheng, L., Chiang, W.-L., Sheng, Y., Zhuang, S., Wu, Z., Zhuang, Y., Lin, Z., Li, Z., Li, D., Xing, E., et al. (2023). Judging llm-as-a-judge with mt-bench and chatbot arena. *Advances in neural information processing systems*, 36:46595–46623.

Zhou, H., Huang, H., Zhao, Z., Han, L., Wang, H., Chen, K., Yang, M., Bao, W., Dong, J., Xu, B., et al. (2026). Lost in benchmarks? rethinking large language model benchmarking with item response theory. In *Proceedings of the AAAI Conference on Artificial Intelligence*, volume 40, pages 35085–35093.

Zhou, J., Lu, T., Mishra, S., Brahma, S., Basu, S., Luan, Y., Zhou, D., and Hou, L. (2023). Instruction-following evaluation for large language models. *arXiv preprint arXiv:2311.07911*.

## A Evaluated LLMs

Table 7 lists all 66 LLMs evaluated in this study, drawn from the HELM Capabilities leaderboard as of May 2025.

## B Distance Distribution Plots

Figures 5, 6, 7 show the distributions of the distance between prompts of the GPQA\_CHUNKED, GPQA\_NOCHUNK and GPQA datasets, respectively, with different models and distance metrics.

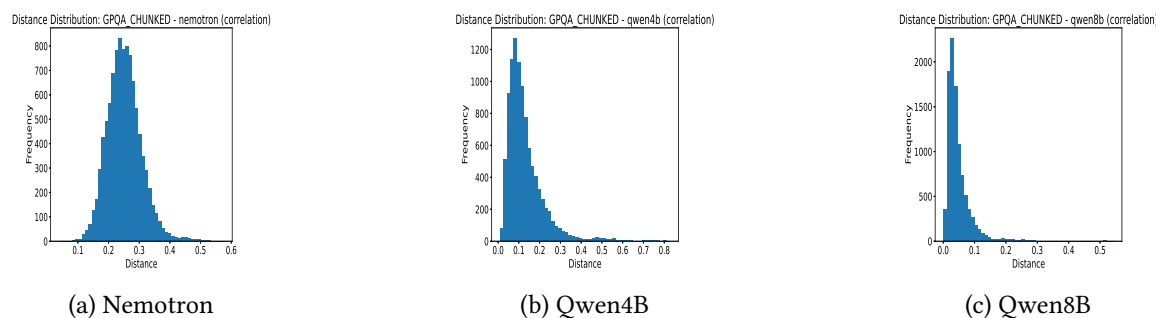


Figure 5: Distance distributions for dataset GPQA\_CHUNKED and different models with selected metrics correlation.

## C Rank shift heatmap for Online-MIS on IFEval (Nemotron, correlation, p80)

Figure 8 presents a rank shift heatmap for the Online-MIS method evaluated on the IFEval benchmark using a Qwen 4B model with cosine similarity at a 20th percentile threshold. Each cell in the heatmap encodes the deviation of a subset’s model ranking from the full-benchmark baseline ranking, with green cells indicating that a model ranked higher in the subset than in the full benchmark and red cells indicating a lower rank. The rightmost column represents the full benchmark ranking itself, showing zero deviation by definition. The seed columns corresponding to different random subsets display highly consistent patterns with one another, as evidenced by a Kendall’s W concordance coefficient of 0.972, meaning the subsets reliably agree on their internal orderings. However, these subset rankings diverge substantially from the full-benchmark baseline, reflected in a Spearman correlation of  $\rho = 0.820$  between the subset and baseline rankings. This particular configuration is highlighted as an extreme case that illustrates the tension between intra-seed

Table 7: List of 66 Models in Omni-MATH Aggregated Benchmark

#	Model Key	Provider
1	amazon_nova_lite	Amazon
2	amazon_nova_micro	Amazon
3	amazon_nova_premier	Amazon
4	amazon_nova_pro	Amazon
5	claude_3_5_haiku_20241022	Anthropic
6	claude_3_5_sonnet_20241022	Anthropic
7	claude_3_7_sonnet_20250219	Anthropic
8	claude_4_opus_20250514	Anthropic
9	claude_4_opus_20250514_extended_thinking_with_thinking	Anthropic
10	claude_4_sonnet_20250514	Anthropic
11	claude_4_sonnet_20250514_extended_thinking_with_thinking	Anthropic
12	claude_4_5_haiku_20251001	Anthropic
13	claude_4_5_sonnet_20250929	Anthropic
14	deepseek_v3	DeepSeek
15	deepseek_r1_0528_with_thinking	DeepSeek
16	gemini_1_5_flash_002	Google
17	gemini_2_0_flash	Google
18	gemini_2_0_flash_lite_02_05_preview	Google
19	gemini_2_5_flash_04_17_preview	Google
20	gemini_2_5_flash_lite	Google
21	gemini_2_5_pro_03_25_preview	Google
22	gemini_3_pro_preview_with_thinking	Google
23	glm_4_5_air_fp8_with_thinking	Zhipu AI
24	gpt_4_1_2025_04_14	OpenAI
25	gpt_4_1_mini_2025_04_14	OpenAI
26	gpt_4_1_nano_2025_04_14	OpenAI
27	gpt_4o_2024_11_20	OpenAI
28	gpt_4o_mini_2024_07_18	OpenAI
29	gpt_5_2025_08_07_with_thinking	OpenAI
30	gpt_5_mini_2025_08_07_with_thinking	OpenAI
31	gpt_5_nano_2025_08_07_with_thinking	OpenAI
32	gpt_5_1_2025_11_13	OpenAI
33	gpt_oss_120b_with_thinking	OpenAI
34	gpt_oss_20b	OpenAI
35	grok_3_beta	xAI
36	grok_3_mini_beta	xAI
37	grok_4_0709	xAI
38	ibm_granite_3_3_8b_instruct	IBM
39	ibm_granite_4_0_micro	IBM
40	ibm_granite_4_0_small	IBM
41	kimi_k2_instruct	Moonshot AI
42	llama_3_1_instruct_turbo_405b	Meta
43	llama_3_1_instruct_turbo_70b	Meta
44	llama_3_1_instruct_turbo_8b	Meta
45	llama_4_maverick_17bx128e_instruct_fp8	Meta
46	llama_4_scout_17bx16e_instruct	Meta
47	marin_8b_instruct	Marin
48	mistral_instruct_v0_3_7b	Mistral AI
49	mistral_large_2411	Mistral AI
50	mistral_small_3_1_2503	Mistral AI
51	mixtral_instruct_8x7b	Mistral AI
52	o3_2025_04_16	OpenAI
53	o4_mini_2025_04_16	OpenAI
54	olmo_2_13b_instruct_november_2024	AllenAI
55	olmo_2_32b_instruct_march_2025	AllenAI
56	olmo_2_7b_instruct_november_2024	AllenAI
57	olmoe_1b_7b_instruct_january_2025	AllenAI
58	palmyra_fin	Writer
59	palmyra_med	Writer
60	palmyra_x5	Writer
61	palmyra_x_004	Writer
62	qwen2_5_instruct_turbo_72b	Alibaba
63	qwen2_5_instruct_turbo_7b	Alibaba
64	qwen3_235b_a22b_fp8_throughput_with_thinking	Alibaba
65	qwen3_235b_a22b_instruct_2507_fp8	Alibaba
66	qwen3_next_80b_a3b_thinking_with_thinking	Alibaba

consistency and cross-baseline distinctiveness: the subsets are highly stable among themselves yet systematically reorder models relative to the full benchmark.

## D Potential risks

**Potential Risks.** We identify four potential risks associated with this work. (1) **Adversarial subset selection.** Although our framework is model-agnostic and selection is driven solely by embedding-space structure, a practitioner could exploit the configurability of the pipeline—choosing embedding model, distance measure, and threshold post hoc—to produce a subset that systematically favours a particular LLM. We recommend that benchmark curators fix and publicly disclose the full configuration (embedding, distance, threshold, solver) before any model evaluation is con-

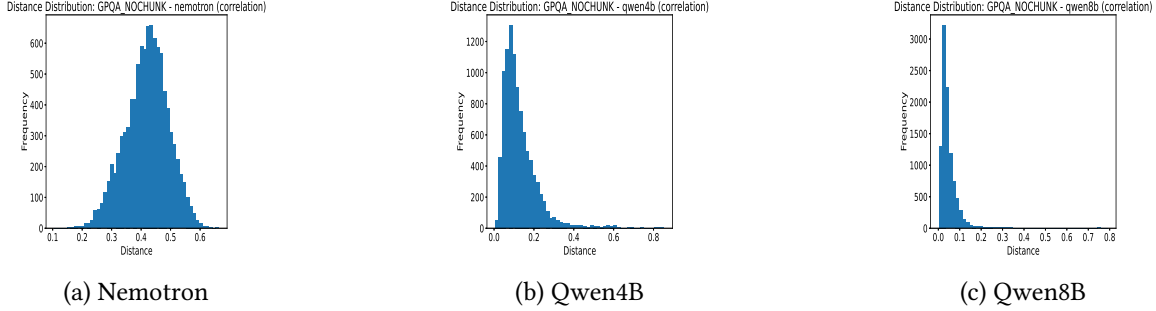


Figure 6: Distance distributions for dataset GPQA\_NOCHUNK and different models with selected metrics correlation.

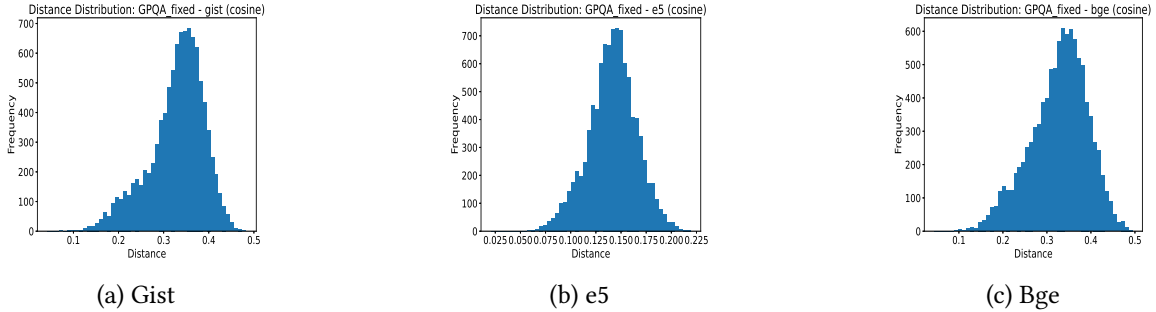


Figure 7: Distance distributions for dataset GPQA and different (small) models with selected metrics cosine.

ducted. (2) **Embedding bias amplification.** MIS selection corrects coverage bias only relative to what the chosen embedding model captures. If the embedding model encodes cultural, linguistic, or domain-specific biases, those biases may be amplified in the selected subset rather than corrected. This risk is highest for domain-specific or multilingual benchmarks, which we have not validated. (3) **Reduced capability coverage.** Aggressively pruned subsets (e.g., at  $p_{10}$ – $p_{20}$ ) may omit prompts that probe rare but important capabilities. This is particularly relevant for safety-critical evaluations, where under-represented edge cases carry disproportionate importance and should not be discarded in favor of coverage uniformity.

## E Computational experiment

**Large Embedding Generation** We generated dense vector representations of each prompt using three encoder models: Qwen3-8B, Qwen3-4B, and Nemotron-8B, all loaded in half-precision (float16) with automatic device placement via HuggingFace Transformers. Model loading was sequential and took approximately 5m43s (Qwen3-8B, 5 shards), 3m14s (Qwen3-4B, 3 shards), and 7m06s (Nemotron-8B, 4 shards) respectively. Each prompt was embedded under two conditions no-chunking and chunked to assess the effect of long-text handling on representation quality. *No-chunk condition.* Each prompt was tokenized with hard truncation at 4,096 tokens and passed through the model in a single forward pass. Token-level hidden states were aggregated via mean pooling over non-padding positions, then L2-normalized to unit length. *Chunked condition.* To avoid information loss from truncation on longer prompts, we applied a sliding-window strategy. Token sequences were split into overlapping windows of 510 tokens (512 minus 2 special tokens) with a stride of 256, yielding 50% overlap between adjacent chunks. Prompts fitting within 510 tokens were passed as a single chunk with no splitting. Each chunk was embedded independently using the same mean-pooling procedure, and the final prompt vector was computed as a length-

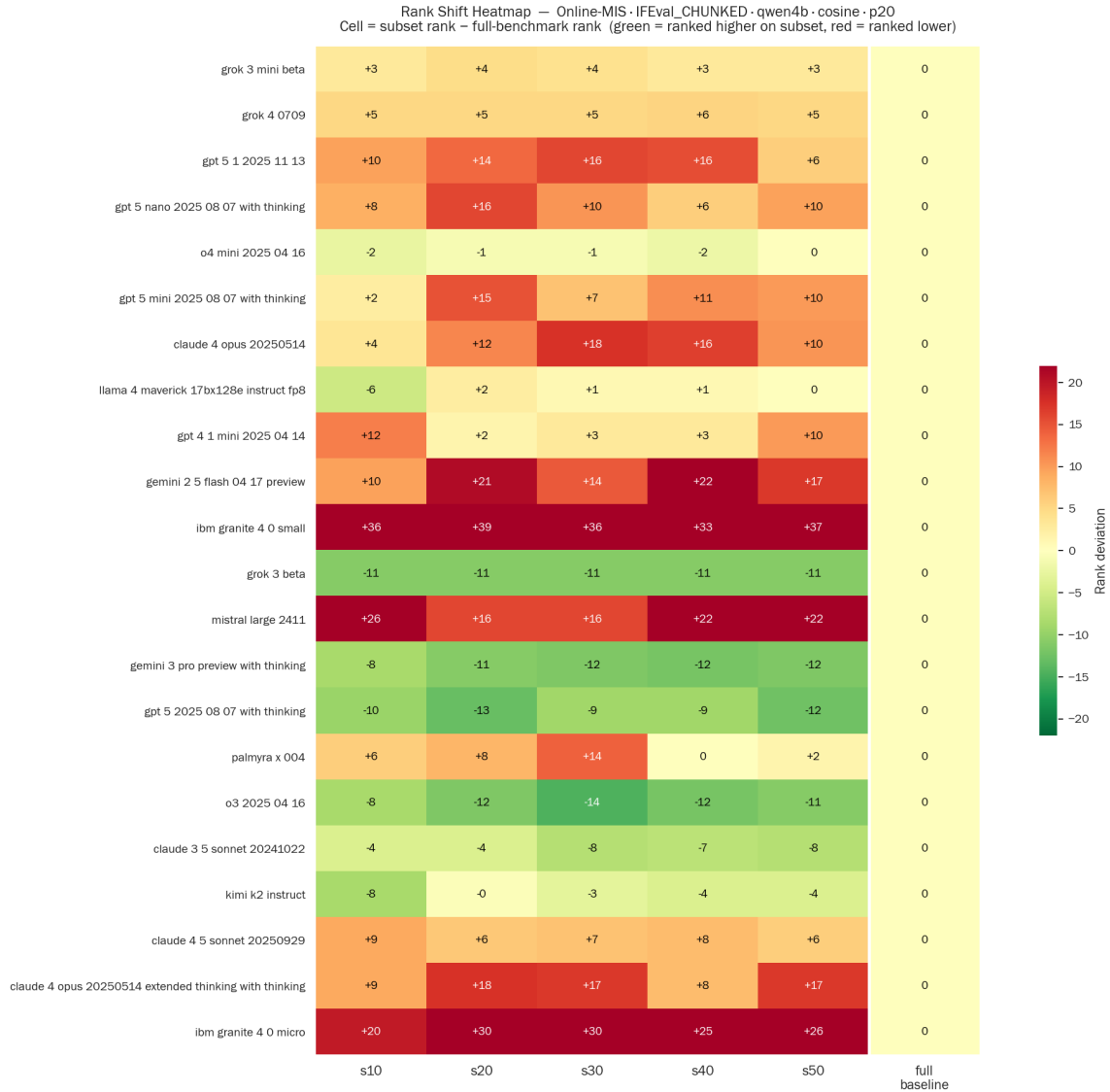


Figure 8: Rank shift heatmap for Online-MIS on IFEval (Qwen4b, cosine, p20). Each cell: deviation of subset rank from full-benchmark baseline rank (green = ranked higher, red = ranked lower). Last column is the full benchmark ranking, which is 0 since it is deviation from itself. Seed columns show similar patterns (consistent,  $W = 0.972$ ) while the ranking differs from the baseline column (distinctive,  $\rho = 0.820$ —an extreme case illustrating maximum distinction).

weighted average across chunks where each chunk’s contribution is proportional to its token count followed by L2 normalization.

Instruction prefix (Nemotron): For Nemotron-8B, each prompt was prepended with the task instruction "Instruct: Represent the following text for clustering: " prior to embedding, following the recommended usage for that model. No prefix was applied for the Qwen models.

Datasets and throughput: The pipeline was applied to all prompts across four benchmarks: GPQA, IFEval, MMLU-Pro, and Omni-MATH. From the execution log, steady-state throughput during the no-chunk pass on GPQA reached approximately 910 items/second for short prompts, with occasional slowdowns to 13 items/second on longer prompts where GPU memory pressure increased processing time. The chunked pass on Omni-MATH the largest dataset with the most

variable prompt lengths ran at a sustained 11 items/second for the bulk of the dataset, with periodic slowdowns at 9098% completion consistent with a small number of unusually long prompts triggering more chunks. Total wall-clock time for the full pipeline across all datasets and conditions was on the order of tens of minutes. Embeddings were written incrementally to JSONL files keyed by prompt ID, with separate output files per dataset, condition, and model.

**Computational Resources and Runtime:** All the experiments for generating the large embeddings were executed on the SLING national HPC infrastructure (Slovensko nacionalno superraznalnisko omreje, Slovenia) on node nsc-vfp004, equipped with 2x NVIDIA L40S GPUs, a 64-core AMD CPU, and 503 GB RAM. The job was allocated all 64 CPUs, 64 GB of system memory, and both GPUs. The full pipeline covering all four datasets, both embedding conditions (no-chunk and chunked), and all three models completed in 52 minutes and 42 seconds of wall-clock time.

**Small Embedding Generation** In addition to the large generative encoders, we computed embeddings using three smaller, dedicated sentence embedding models: BGE-large-en-v1.5 (BAAI), E5-large (intfloat), and GIST-small-Embedding-v0 (avsolatorio). These models were run locally on a Lenovo ThinkPad equipped with an Intel Core Ultra 7 258V CPU, 32 GB RAM, and an Intel Arc 140V GPU with 16 GB VRAM.

Each model uses a task-specific instruction prefix prepended to the prompt text: BGE uses "Represent this sentence for searching relevant passages: ", E5 uses "query: ", and GIST uses no prefix. The same chunked embedding strategy was applied as for the large models, with a maximum chunk size of 510 tokens (512 minus 2 special tokens) and no overlap between chunks (stride equals chunk size). For prompts fitting within 510 tokens, no splitting was applied. Chunks were decoded back to text before re-tokenization, to ensure compatibility with BERT-style tokenizers. The same length-weighted aggregation and L2 normalization were applied to produce the final embedding. Prompts exceeding 510 tokens triggered a logged warning during processing.

For the smaller encoder models, non-overlapping chunks were used, as their 512-token context limit leaves minimal headroom for redundant overlap. For the large models, a 50% overlap (stride of 256 tokens) was applied to better preserve context across chunk boundaries, taking advantage of their larger 4,096-token capacity. The pipeline was run separately for each of the four datasets (GPQA, IFEval, MMLU-Pro, Omni-MATH), producing one JSONL output file per dataset.

**Optimization Algorithms Experiments** The optimization algorithms experiments were conducted on the VEGA high-performance computing supercomputer hosted at the Institute of Information Science (IZUM), Maribor, Slovenia. VEGA is a EuroHPC petascale system based on the *Atos BullSequana XH2000* architecture, consisting of 960 CPU nodes equipped with dual-socket AMD EPYC 7H12 processors running at 2.6 GHz. Standard CPU nodes provide 256 GB RAM, while a subset of large-memory nodes provides up to 1 TB RAM. The system uses a high-speed HDR100 InfiniBand interconnect and is managed through the SLURM workload scheduler.

All MIS-related experiments were executed in a single-threaded configuration for fair comparison across algorithms. The evaluated methods include:

- CPLEX (exact branch-and-bound optimization),
- GREEDY (deterministic heuristic),
- Online-MIS (stochastic online independent set heuristic),
- ReduMIS (kernelization and local-search based stochastic solver).

Each job was allocated 32 GB RAM and a maximum execution time limit of 600 seconds. Stochastic algorithms (Online-MIS and ReduMIS) were executed using multiple random seeds.

## F AI Assistants in Research or Writing

AI writing assistance (Claude, Anthropic) was used solely for grammar and language checking; all scientific content and conclusions are the authors' own.

## G How Benchmarks Differ in Subset Characteristics

Table 8: Distribution of subset configurations by consistency and distinctiveness category.

<b>Benchmark</b>	<b>Representative</b> ( $W \geq 0.90$ & $\rho \geq 0.95$ )	<b>Distinctive</b> ( $W \geq 0.90$ & $\rho < 0.95$ )	<b>Inconsistent</b> ( $W < 0.90$ )
GPQA	80.9%	19.1%	0.0%
IFEval	59.6%	39.8%	0.6%
MMLU-Pro	97.4%	2.6%	0.0%
Omni-MATH	98.1%	1.9%	0.0%